**Supplementary Materials and Methods:**

**Survival analysis**

The separation of high and low *CD177* groupings were based on the optimal cut-off function of the survminer R package, with the minimal proportion comparison for each cohort set to 15% versus 85% of the total samples. HR and –log10(*P* values) were graphed with R studio and ggplots2.

**Cell lysates, immunoprecipitation and immunoblots**

Cells were lysed in cell lysis buffer (50 mM Trish-HCl pH 7.5, 1 mM EDTA, 1mM EGTA, 1% Triton-X100, 100 mM KCl, 50 mM NaF, 10 mM Na 2-glycercophosphatem 1mM $Na_3VO_4$, 100 nM aprotinin, 1 μM bestatin, 1 μM pepstatin A supplemented with 0.1% sodium dodecyl sulfate (SDS) for immunoblots or without for immunoprecipitation).

Antibodies were anti-CD177 (4c4; Sigma Aldrich) anti-CD177 (N3c3; GeneTex, Irvine, CA), anti-E-Cadherin (G010; Santa Cruz Biotechnology, Santa Cruz, CA), anti-Actin and anti-β-Catenin (E-5 Santa Cruz Biotechnology), anti-GAPDH, anti-Flotillin-2 and anti-α-Tubulin (DM1a; Cell Signaling Technologies, Danvers, MA).

**Immunohistochemistry**

Formalin fixed tissues were processed by the University of Iowa Pathology core. Sections were deparaffinized in a series of xylene washes and rehydrated with ethanol and water. CD177 IHC images were taken from the Human Protein Atlas. Specific images used are as follows: cervical cancer HPA046601 (Cervix T-83000) patient ID 3400 and 4224 (www.proteinatlas.org/ENSG00000204936-CD177/pathology/tissue/cervical+cancer); prostate cancer HPA04660 (ProstateT-77100) patient ID 4158 and 4172 (www.proteinatlas.org/ENSG00000204936-CD177/pathology/tissue/prostate+cancer); LSCC HPA041820 (T-28000) patient ID 2779 and 1937 (https://www.proteinatlas.org/ENSG00000204936-CD177/pathology/tissue/lung+cancer). CD177 IHC images for cervical cancer, prostate cancer and LSCC are available from Human Protein Atlas (www.proteinatlas.org).

**Supplementary Table S1-S4**

**Table S1.** Correlation between expression of various CD molecules and relapse-free survival (RFS) in human breast cancer.

| CD molecule | Logrank P | HR | HR range | RFS |
|---|---|---|---|---|
| CD34 | 0 | 0.6 | 0.53-0.68 | + |
| CD11b | 0 | 0.57 | 0.51-0.65 | + |
| CD62-P | 0 | 0.52 | 0.46-0.59 | + |
| CD177 | 8.90E-15 | 0.62 | 0.55-0.7 | + |
| CD314/NKG2D | 2.40E-13 | 0.65 | 0.58-0.73 | + |
| CD31 | 5.00E-12 | 0.67 | 0.6-0.75 | + |
| CD94 | 2.60E-11 | 0.64 | 0.56-0.73 | + |
| CD8 | 2.80E-11 | 0.68 | 0.56-0.75 | + |
| CD5 | 7.80E-11 | 0.68 | 0.61-0.77 | + |
| CD4 | 9.20E-09 | 0.7 | 0.62-0.79 | + |
| CD271 | 3.20E-08 | 0.73 | 0.65-0.81 | + |
| CD68 | 2.60E-06 | 0.76 | 0.68-0.85 | + |
| CD83 | 7.30E-06 | 0.77 | 0.68-0.86 | + |
| CD163 | 1.90E-05 | 1.3 | 1.15-1.46 | - |
| CD40 | 4.30E-05 | 0.79 | 0.7-0.88 | + |
| CD133 | 6.60E-05 | 1.3 | 1.14-1.47 | - |

KMPlot (http://kmplot.com/analysis/index.php?p=service&cancer=breast) was used to calculate Logrank *P* values and other information. CD, clustering differentiation; HR, hazard ratio; RFS, relapse-free survival. +, positive correlation between CD expression and RFS; -, negative correlation between CD expression and RFS.

**Table S2.** Correlation between *CD177* expression and survival in several solid tumors.

| Cancer | Subtype | HR | HR (range) | Logrank *P* | N | source |
|---|---|---|---|---|---|---|
| Breast (RFS) | all | 0.62 | 0.55-0.7 | 8.90E-15 | low: 928<br>high: 2626 | KMplot |
| | Luminal A | 0.67 | 0.56-0.8 | 7.00E-48 | low:871<br>high: 893 | KMplot |
| | Luminal B | 0.73 | 0.59-0.91 | 0.005 | low: 656<br>high: 346 | KMplot |
| | HER2 | 0.49 | 0.33-0.83 | 0.00071 | low: 80<br>high: 128 | KMplot |
| | Basal-like | 0.62 | 0.48-0.81 | 0.00035 | low: 251<br>high; 329 | KMplot |
| Cervical (OS) | | 0.44 | 0.23-0.83 | 0.0008 | low: 69<br>high: 226 | TCGA |
| LUSC (RFS) | | 0.6 | 0.37-0.98 | 0.0164 | low: 82<br>high: 344 | TCGA |
| Prostate (RFS) | | 0.52 | 0.30-0.89 | 0.0204 | low: 240<br>high: 242 | TCGA |

Summary of data presented in Figure 1C showing correlation between *CD177* expression and survival in several solid tumors. Survival curves were generated using the cutoff for high and low *CD177* expression which generated the best separation between the two groups. OS: overall survival. LUSC, lung squamous cell carcinoma.

**Table S3.** Correlation between *CD177* expression and overall survival in 30 cancer types deposited in the TCGA. Data used to generate Figure S1C.

| Cancers | Abbrev. | HR | Pval | Size | High | Low |
|---|---|---|---|---|---|---|
| Adrenocortical Carcinoma | ACC | 0.236 | 0.020 | 79 | 18 | 61 |
| Bladder Carcinoma | BLCA | 1.596 | 0.060 | 407 | 345 | 62 |
| Breast invasive Carcinoma | BRCA | 1.375 | 0.054 | 1095 | 543 | 552 |
| Cervical squamous cell carcinoma | CESC | 0.396 | 0.001 | 303 | 235 | 68 |
| Cholangiocarcinoma | CHOL | 2.079 | 0.146 | 36 | 19 | 17 |
| Colon adenocarcinoma | COAD | 0.329 | 0.010 | 286 | 53 | 233 |
| Diffuse large B cell lymphoma | DLBCL | 2.864 | 0.198 | 48 | 25 | 23 |
| Glioblastoma Multiforme | GBM | 1.200 | 0.337 | 158 | 98 | 60 |
| Head and neck squamous cell carcinoma | HNSC | 0.558 | 0.008 | 519 | 90 | 429 |
| Kidney Chromophobe | KICH | 0.267 | 0.049 | 66 | 55 | 11 |
| Kidney renal clear cell carcinoma | KIRC | 1.347 | 0.138 | 533 | 419 | 114 |
| Kidney renal papillary cell carcinoma | KIRP | 2.252 | 0.007 | 290 | 82 | 208 |
| Lower grade glioma | LGG | 0.668 | 0.144 | 516 | 77 | 439 |
| Liver hepatocellular carcinoma | LIHC | 1.522 | 0.061 | 371 | 58 | 313 |
| Lung adenocarcinoma | LUAD | 0.747 | 0.111 | 511 | 423 | 88 |
| Lung Squamous cell carcinoma | LUSC | 0.660 | 0.044 | 502 | 77 | 425 |
| Mesothelioma | MESO | 0.692 | 0.177 | 87 | 23 | 64 |
| Ovarian Cancer | OV | 1.574 | 0.030 | 262 | 40 | 222 |
| Pancreatic ductal adenocarcinoma | PAAD | 2.144 | 0.024 | 178 | 152 | 26 |
| Pheochromocytoma and paraganglioma | PCPG | 2.944 | 0.237 | 179 | 60 | 119 |
| Prostate adenocarcinoma | PRAD | 0.186 | 0.034 | 497 | 308 | 189 |
| Rectal adenocarcinoma | READ | 0.302 | 0.021 | 94 | 80 | 14 |
| Sarcoma | SARC | 0.606 | 0.083 | 258 | 50 | 208 |
| Skin cutaneous melanoma | SKCM | 2.953 | 0.009 | 103 | 17 | 86 |
| Testicular germ cell cancer | TGCT | 5.185 | 0.157 | 150 | 57 | 93 |
| Thyroid cancer | THCA | 2.848 | 0.053 | 505 | 213 | 292 |
| Thymoma | THYM | 0.000 | 0.999 | 119 | 22 | 97 |
| Uterine corpus endometrial cancer | UCEC | 1.935 | 0.069 | 174 | 85 | 89 |
| Uterine carcinosarcoma | UCS | 3.940 | 0.061 | 57 | 47 | 10 |
| Uveal melanoma | UVM | 0.518 | 0.121 | 80 | 53 | 27 |

**Table S4.** RNA sequencing data showing fragments per kb of transcript per million mapped reads (FPKM). 5 *Cd177*$^{+/-}$(WT1-5) and 7 *Cd177*$^{-/-}$ (KO1-7) tumors from Figure 3D-E were included. Shown as EXCEL file.

**Supplementary Figure S1-S6.**

**Figure S1 related to Figure 1:** CD177 is commonly lost in invasive cancer and positively correlated with survival**.**

(A-B) Correlation between *CD177* expression and site-specific metastasis-free survival. Data from GSE2034 (A; n=145 low; n=141 high) and GSE2603 (B; n=41 low; n=40 high). Logrank test was done to determine significance.

(C) Correlation between *CD177* expression and overall survival in 30 cancer types from the TCGA. Hazard ratios and *P* value are bases on the optimal cut-off for low and high *CD177* expression with a minimal proportion for each cohort of 15% versus 85% of the total samples. Graph depicts the Log2 hazard ratio versus –Log10 *P* value. N numbers and abbreviations are provided in Table S3.

(D-F) IHC staining images for CD177 in cervical cancer (D), prostate cancer (E) and lung squamous cell carcinoma (LUSC, F). One negative (left) and one positive (right) image are shown for each. The zoom-in images showed the CD177 expression on membrane of epithelial cells.

**Figure S2 related to Figure 1:** CD177 is commonly lost in invasive cancer**.**

(A) Immunofluorescent images for CD177 in human breast cancer samples (BrCa, bottom) and paired normal samples (top). Tumor area is outlined in yellow.

(B) *CD177* expression relative to *Ppia* as fold changes compared to HMLE in the indicated cell lines.

(C) The indicated cell lines were grown in 3-dimensional cultures in poly-HEMA coated plates and flow cytometry was performed to determine surface CD177 expression. Graph depicts the percentages of $CD177^{+}$ cells.

(D) Flow cytometry for surface CD177 in tamoxifen-resistant MCF7R and parental MCF7 cells.

(E) Table summarizing the expression of CD177, E-Cadherin, and β-Catenin protein in cell lines.

(F) Log2 *CD177* expression versus promoter methylation (average β-values) in normal mammary gland (blue) and breast cancer (red). Data from TCGA invasive ductal breast carcinoma.

**Figure S3 related to Figure 2:** CD177-deficiency leads to proliferative mammary epithelial cells

(A-E). The No. 4 mammary glands from the indicated mice were collected at 10 months of age from WT or *Cd177*$^{-/-}$ females and paraffin embedded. Tissue sections were subject to H & E staining (A), Ki-67 (B, upper panels), Krt-5 (B, lower panels), PR and ER (C). Percentages of Krt-5 (D) or Krt-8 (E) positive cells were calculated based on IHC images.

**Figure S4 related to Figures 3-4: CD177 suppresses breast cancer.**

(A) *Cd177* expression was determined by real-time PCR from 67NR cells used in Figure 3E and 4C. Graph depicts the average *Cd177* expression relative to *Peptidylprolyl Isomerase A* (*Ppia*) as a fold change compared to 67NR control cells ± s.d. (n=3).

(B) Control or sh1 67NR cells were transiently transfected with empty plasmid (EP) or plasmid encoding human CD177 gene (hCD177). 48 hrs later, cells were collected for flow cytometry for surface expression of human CD177. Note that anti-human CD177 (MEM166) does not recognize mouse CD177.

(C) *MMTV-ErbB2/Cd177*$^{+/-}$ and *MMTV-ErbB2/Cd177*$^{-/-}$ mice were monitored for tumor development. Graph depicts a Kaplan-Meier curve for tumor onset (days when first tumor developed) for the indicated mice. Logrank test was used to determine significance.

(D) IHC staining of CD177 on *MMTV-ErbB2* tumors at low magnification, related to Figure 4F.

(E) Representative Ki-67 staining of tumors from *MMTV-ErbB2/Cd177*$^{+/-}$ and *MMTV-ErbB2/Cd177*$^{-/-}$ mice.

(F) Graph depicts the average number of Ki-67$^{+}$ cells from (E) ± s.d. 3 images per section were counted (n=3). One-way ANOVA was used to determine significance.

**Figure S5 related to Figure 5: CD177 attenuates the canonical WNT/β-Catenin signaling**

(A). Left panel: RNAseq was performed using tumor RNAs collected from *MMTV-ErbB2/Cd177*$^{+/-}$ and *MMTV-ErbB2/Cd177*$^{-/-}$ mice used in Figure 6C. Graph depicts the average *Cd177* mRNA level as FPKM ± s.d. from *MMTV-ErbB2/Cd177*$^{+/-}$ and *MMTV-ErbB2/Cd177*$^{-/-}$ mice. Right panel: Real-time PCR confirming the *Cd177* expression in RNAseq specimens. Graph depicts the average *CD177* mRNA level relative to *Ppia* ± s.d.

Students t test was used to determine significance. Related to Figure 5C. 5 for *MMTV-ErbB2/Cd177*$^{+/-}$ and 7 for *MMTV-ErbB2/Cd177*$^{-/-}$ tumors.

(B) TOPflash dual-luciferase assay for β-Catenin activation in H146 cells transfected with siRNA targeting CD177 (siCD177) or control siRNA (siControl), then grown as 3-dimensional colonies in poly-HEMA coated plates. Cells were treated with or without 400 ng/ml recombinant Wnt3a for 24 hr. Left panel: Immunoblotting for CD177 and Actin. Right panel: Graph depicts the average firefly luciferase intensity as a fold change compared to untreated control ± s.d. One-way ANOVA with multiple comparisons correction using Dunnett's test was used to determine significance (n=3-6 for all experiments).

(C) Immunoblot for E-cadherin, CD177 and Actin in lysates from Figure 5H: TOPflash dual-luciferase assay for β-Catenin activation in MDA-MB-436 cells transfected with 1) pcDNA3.1 empty vector (control), 2) CD177 and pcDNA3.1, 3) E-cadherin and pcDNA3.1 or 4) both E-cadherin and CD177, treated with or without 400 ng/ml recombinant Wnt3a for 24 hr.

(D) 67NR-sh1 cells from Figure 3E were transiently transfected with control or β-Catenin siRNA. 48 hrs later, cells were either subject to either lysate collection for SDS-PAGE and Western Blotting (left panels), or for in vitro soft agar colony assay (right panels, n = 3 with 2-3 fields counted/repeat).

**Figure S6 related to Figure 6:** CD177 indirectly interacts with β-Catenin.

(A) SKBR3 cells stably expressing CD177 or control (Con) vector were stained for CD177. Immunofluorescent image showing membrane localization of CD177.

(B) Normal human breast tissues were stained with mouse and rabbit IgGs as isotype negative controls for immunofluorescent staining, related to Figure 6A-D.

(C) Human breast tissues were stained for CD177 (green) and E-Cadherin (red). Representative confocal images are shown as individual colors and an overlay.

(D-E) 1 μg of FC-fusion CD177 and His-Tag full-length β-Catenin, both purified from HEK293T cells, were incubated using RIPA buffer, with or without the presence of 1 mg of control or E-Cadherin-depleted cell lysates from HEK293T (D). Note that 1 mg of HEK293T cell lysate was pre-treated with mIgG, a non-relevant

anti-DSG2 antibody, or anti-E-Cadherin antibody, following protein A agarose to deplete E-Cadherin from lysates. Depletion efficiency was determined using Western Blotting of E-Cadherin-depleted cell lysate (E, upper panel) or immunoprecipitates (E, lower panel). (D) Ni-NTA agarose was used to pull down His-β-Catenin complex, following with SDS-PAGE and Western Blotting. Related to Figure 6E.

**Figure S1**

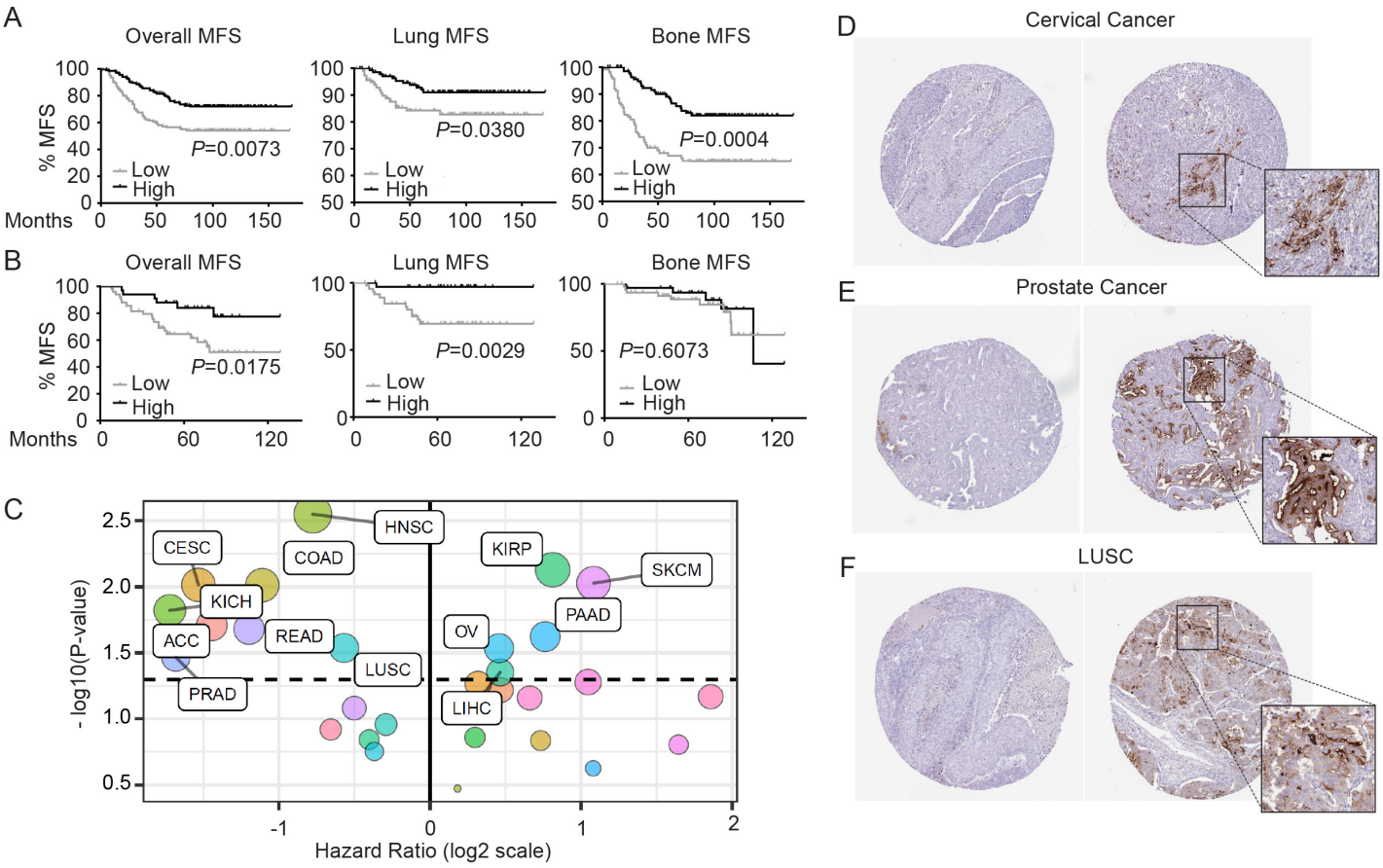
A
Overall MFS
Lung MFS
Bone MFS
% MFS
P=0.0073
P=0.0380
P=0.0004
Low
High
Months
B
Overall MFS
Lung MFS
Bone MFS
P=0.0175
P=0.0029
P=0.6073
C
- log10(P-value)
Hazard Ratio (log2 scale)
HNSC
CESC
COAD
KIRP
SKCM
KICH
PAAD
ACC
READ
OV
LUSC
PRAD
LIHC
D
Cervical Cancer
E
Prostate Cancer
F
LUSC

**Figure S2**

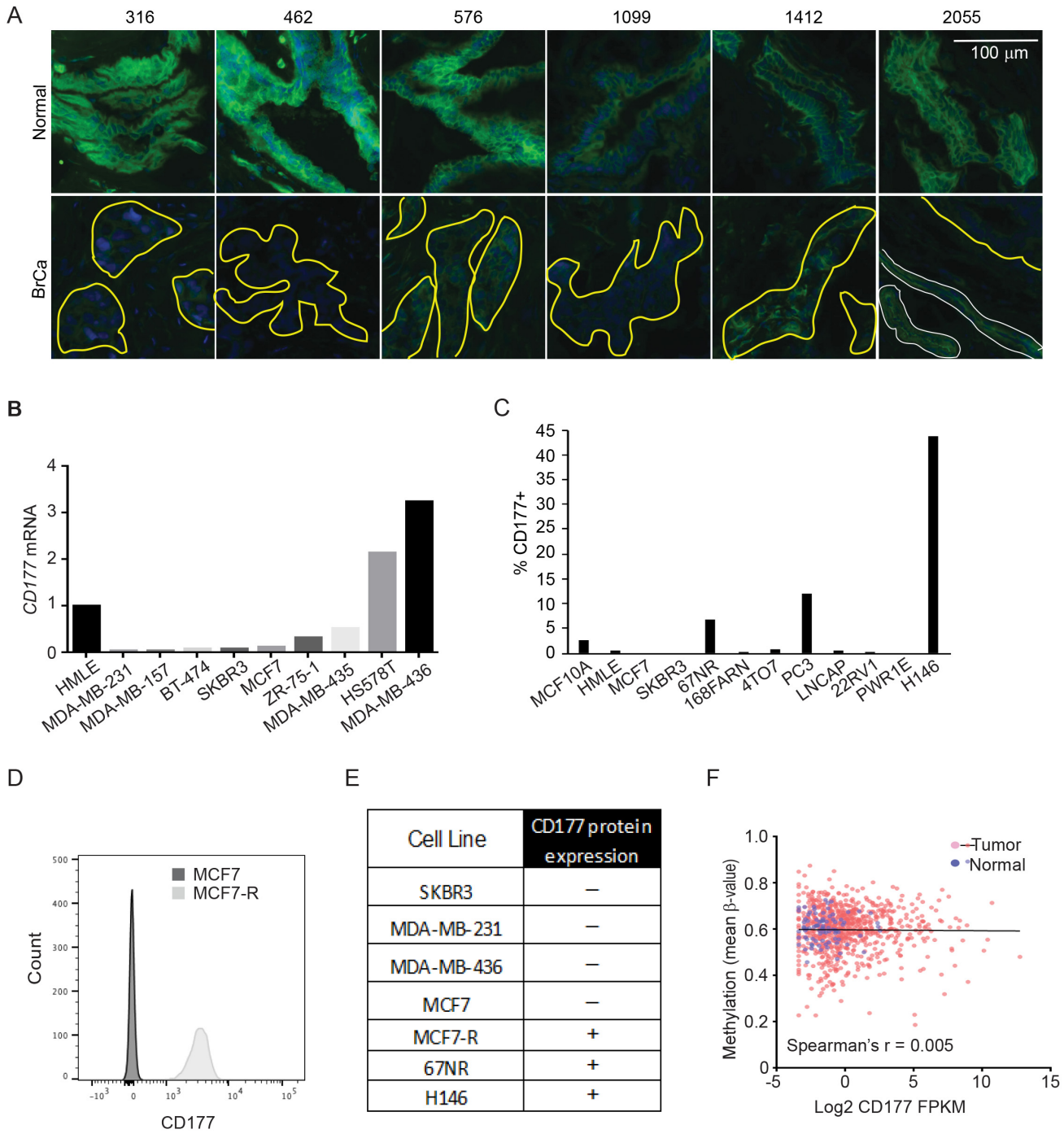


| Cell Line | CD177 protein expression |
|---|---|
| SKBR3 | – |
| MDA-MB-231 | – |
| MDA-MB-436 | – |
| MCF7 | – |
| MCF7-R | + |
| 67NR | + |
| H146 | + |

**Figure S3**

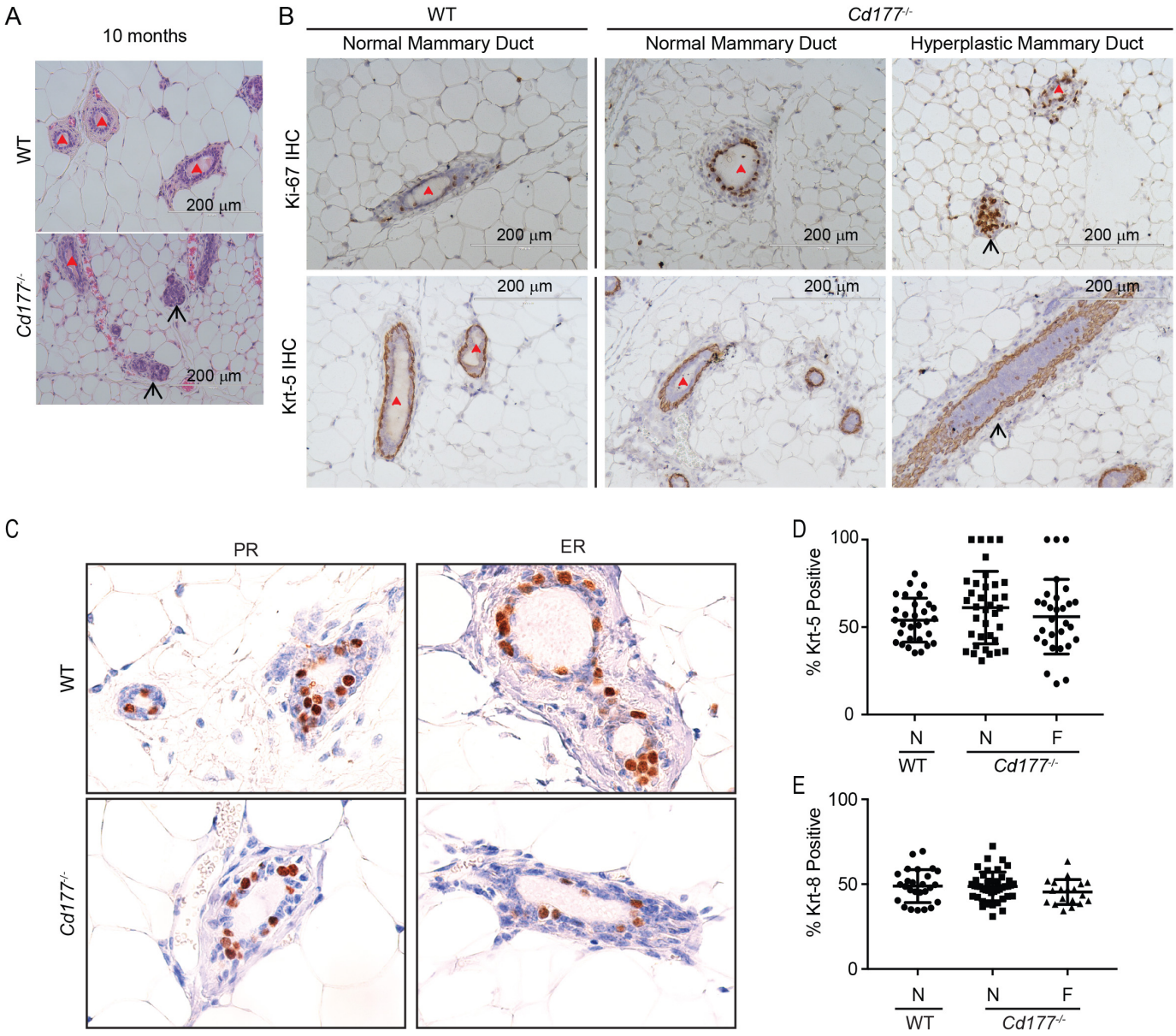
A
10 months
WT
Cd177-/-
200 μm
B
WT
Cd177-/-
Normal Mammary Duct
Normal Mammary Duct
Hyperplastic Mammary Duct
Ki-67 IHC
Krt-5 IHC
200 μm
C
PR
ER
WT
Cd177-/-
D
% Krt-5 Positive
100
50
0
N
N
F
WT
Cd177-/-
E
% Krt-8 Positive
100
50
0
N
N
F
WT
Cd177-/-

**Figure S4**

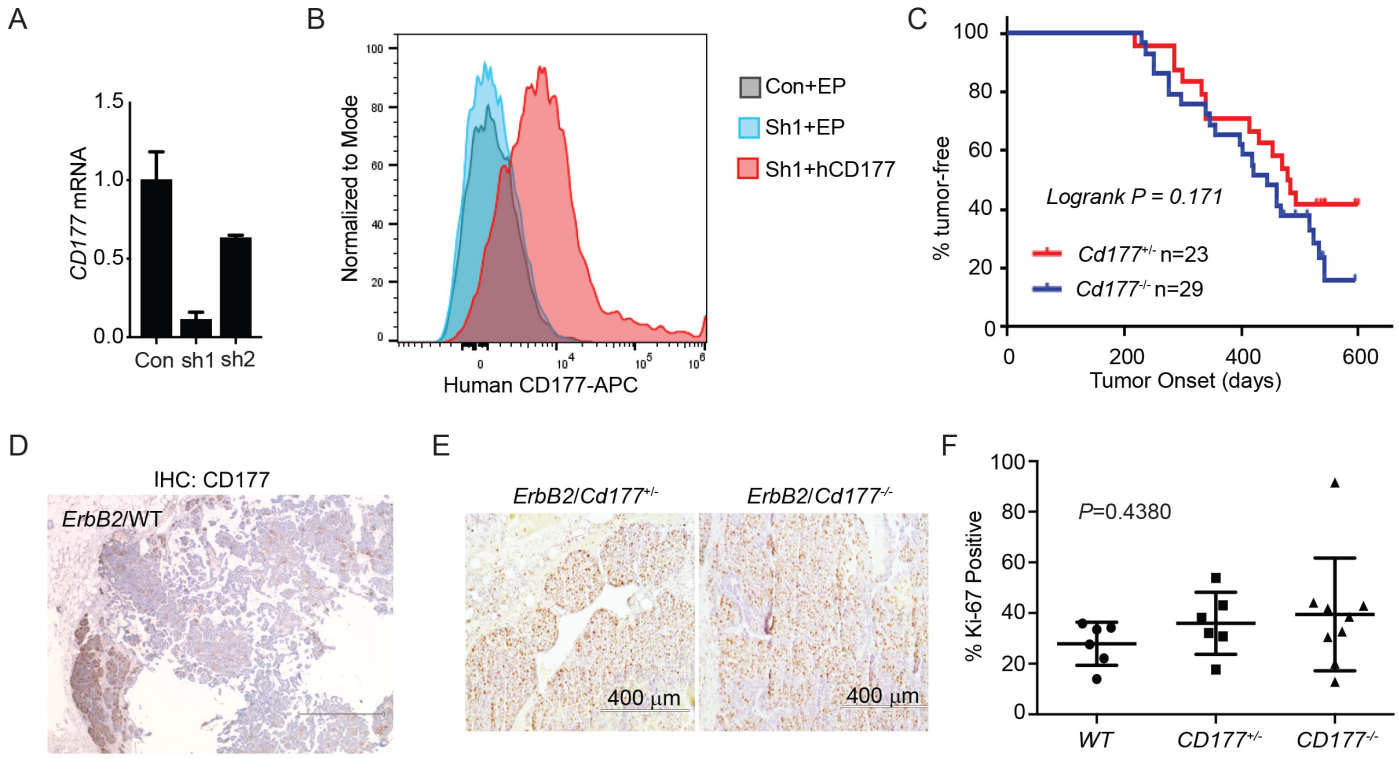
A
CD177 mRNA
1.5
1.0
0.5
0.0
Con sh1 sh2
B
Normalized to Mode
Human CD177-APC
Con+EP
Sh1+EP
Sh1+hCD177
C
% tumor-free
Logrank P = 0.171
Cd177+/- n=23
Cd177-/- n=29
Tumor Onset (days)
D
IHC: CD177
ErbB2/WT
E
ErbB2/Cd177+/-
ErbB2/Cd177-/-
400 μm
400 μm
F
% Ki-67 Positive
P=0.4380
WT
CD177+/-
CD177-/-

**Figure S5**

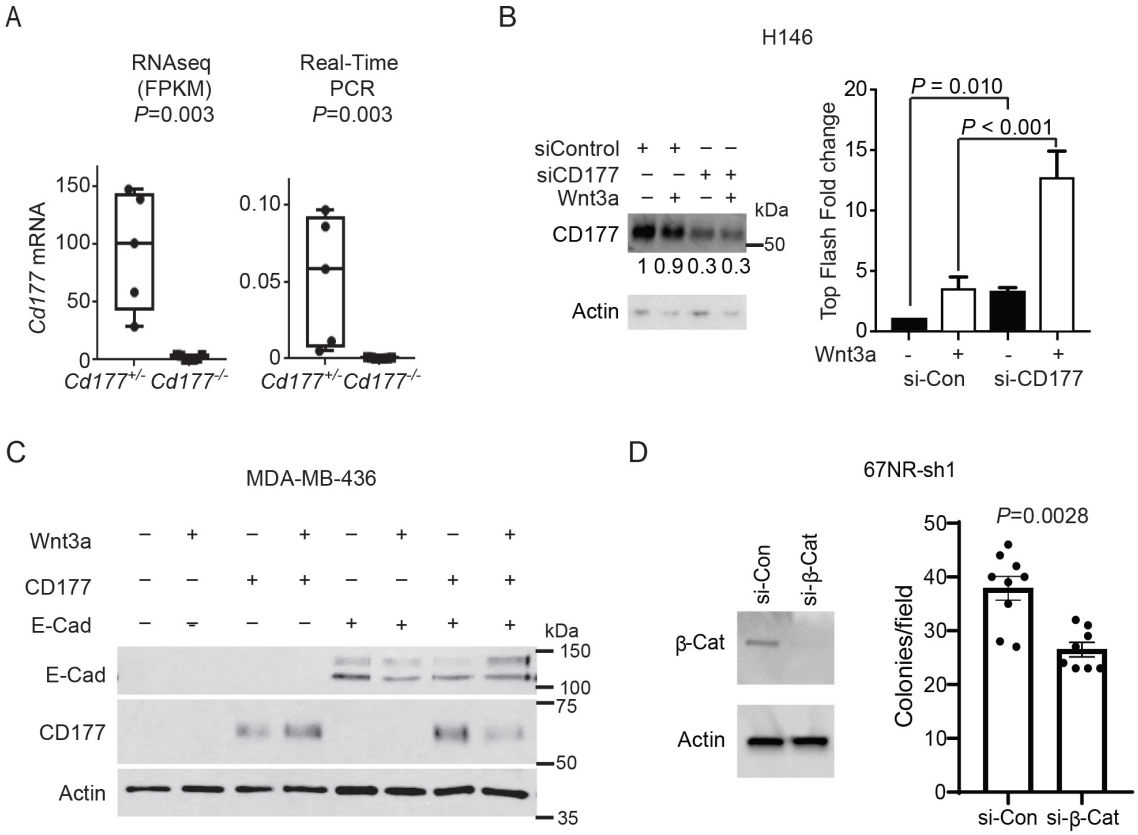
A
RNAseq
(FPKM)
P=0.003
Real-Time
PCR
P=0.003
Cd177 mRNA
150
100
50
0
0.10
0.05
0
Cd177+/- Cd177-/-
Cd177+/- Cd177-/-
B
H146
siControl + + − −
siCD177 − − + +
Wnt3a − + − +
kDa
CD177
50
1 0.9 0.3 0.3
Actin
P = 0.010
P < 0.001
Top Flash Fold change
20
15
10
5
0
Wnt3a - + - +
si-Con
si-CD177
C
MDA-MB-436
Wnt3a − + − + − + − +
CD177 − − + + − − + +
E-Cad − − − − + + + +
kDa
E-Cad
150
100
CD177
75
50
Actin
35
D
67NR-sh1
si-Con
si-β-Cat
β-Cat
Actin
P=0.0028
Colonies/field
50
40
30
20
10
0
si-Con si-β-Cat

Figure S6

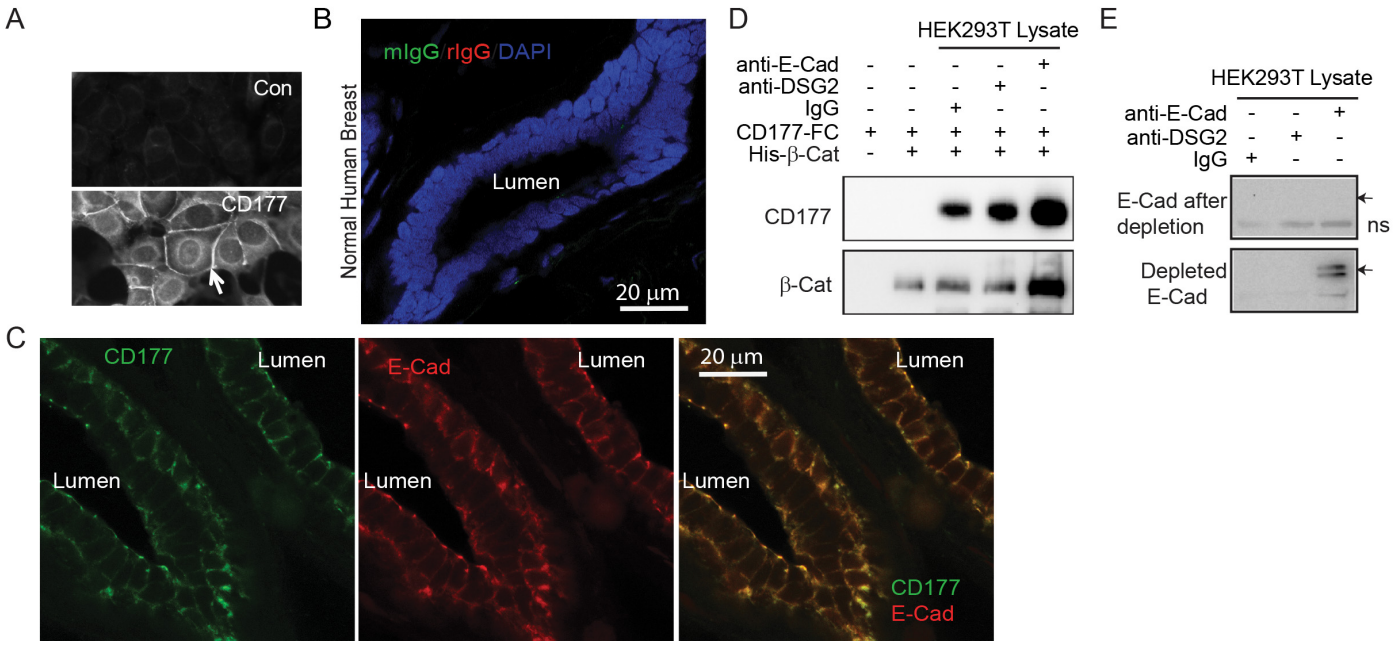
A
Con
CD177
B
mIgG rIgG DAPI
Normal Human Breast
Lumen
20 μm
D
HEK293T Lysate
anti-E-Cad - - - - +
anti-DSG2 - - - + -
IgG - - + - -
CD177-FC + + + + +
His-β-Cat - + + + +
CD177
β-Cat
E
HEK293T Lysate
anti-E-Cad - - +
anti-DSG2 - + -
IgG + - -
E-Cad after depletion
ns
Depleted E-Cad
C
CD177
Lumen
Lumen
E-Cad
Lumen
Lumen
20 μm
Lumen
Lumen
CD177
E-Cad